Soft Matter

Dynamic Article Links

Cite this: *Soft Matter*, 2011, **7**, 4425

www.rsc.org/softmatter

PAPER

Ethanol induces condensation of single DNA molecules

Yanwei Wang,[ab] Shiyong Ran,[a] Baoyuan Man[b] and Guangcan Yang*[a]

Received 4th November 2010, Accepted 25th February 2011
DOI: 10.1039/c0sm01251c

As a widely used precipitation agent for DNA extraction, ethanol is used to induce single molecule DNA condensation. This process is studied with force-measuring magnetic tweezers and atomic force microscopy (AFM). Our experiments provide direct evidence of the metastable intermediate racquet states in DNA collapse induced by ethanol. The measured condensing force is less than 0.2 pN even at 50% ethanol concentration, which is much less than those induced by multivalent cations and cationic surfactants. We confirmed the A-B transition of DNA in ethanol and found that the tensile modulus of A-form DNA is larger than that of B-form. The single molecule pulling experiment shows very different features of neutral ethanol from those of multivalent cations. The pulling curve contains a wide range of step sizes, ranging from tens of nanometres to a few micrometres, contrasting with the relatively uniform interval (about 200 nm) in multivalent cations. Meanwhile, the persistence length of DNA decreases monotonically with the increasing ethanol concentration. The condensing morphologies by the weak attraction of DNA segments in the less polar solvent are loose and flowerlike structures composed of many annealed irregular racquets. The analysis of pulling experiments is supported by AFM direct imaging. We concluded that the dominant factor in DNA condensation induced by ethanol is solvent exclusion rather than the charge neutralization correlation effect.

1. Introduction

DNA condensation is an important process for its high density packing in biological systems, particularly in viruses and sperm cells,[1,2] and has found applications (either by design or serendipity) in artificial gene delivery.[3] In this process, DNA undergoes a dramatic condensation to a compact structure in the presence of various agents, such as multivalent cations,[4–8] alcohol,[9] basic proteins,[10] neutral crowding polymers,[11–16] cationic liposomes[17,18] and anti-cancer drugs.[19] This phenomenon has drawn considerable attention and induced related studies in different fields during the past decades, especially by the recent developed single molecule techniques.

The single molecule approaches allow us to study the behavior of biological macromolecules under applied tensions; the mechanical properties of these molecules help us understand how they function in the cell. They can usually be classified by two major categories: mechanical force transducers and external field manipulators. In the mechanical force transducers—the AFM, microneedles and optical fibers—forces are applied or sensed through bendable beams. In the external field manipulators—optical tweezers (OT), magnetic tweezers (MT), and flow fields—the molecule is acted upon from a distance, by application of external fields (photonic, magnetic, or hydrodynamic) either to the molecule itself or to an appropriate handle to which the molecule is attached. Among them, single molecule magnetic tweezers are a versatile and inexpensive instrument. This technique allows the application of a constant pulling force on a single DNA molecule while measuring its elongation in real time. For instance, Fu *et al.*[20] studied the compaction dynamics of single DNA molecule invoked by hexammine cobalt chloride. The observations suggested that the folding/unfolding process is a reversible transition between two metastable structural states. However, Besteman *et al.*[21] investigated DNA condensation by cobalt sepulchrate, and showed that condensation of DNA under tension is an activated process that is irreversible on experimental time scales. Effect of DNA-binding proteins such as HU, IHF and H-NS on DNA mechanical properties have also been measured with magnetic tweezers at single-molecule level.[22–24] Besides, Baumann *et al.*[4] used laser tweezers to determine the elastic properties of DNA as a function of ionic strength. Hud's group[25,26] found that an initial static loop plays an important role in the nucleation and growth of DNA condensation and the condensates are salt dependent. On the other hand, Yoshikawa group[27,28] investigated the phenomenon of the intrachain segregation on DNA and found it is condensing agent dependent.

Two different mechanisms have been proposed to explain the condensation induced by multivalent cations and poor solvents like ethanol.[9] The former neutralize 90% of the charge of DNA and screen the Coulombic repulsion between the DNA

[a]*School of Physics and Electronic Information, Wenzhou University, Wenzhou, 325035, China. E-mail: yanggc@wzu.edu.cn; Fax: +86-577-86689010; Tel: +86-577-86689033*
[b]*School of Physics and Electronic Sciences, Shandong Normal University, Jinan, 250014, China*

phosphates to produce the attraction through the correlated fluctuations of the ion atmosphere.[29,30] On the other hand, poor solvents of nucleic acids make interactions of DNA with its environment less favorable. Due to its semiflexible properties, the collapse of DNA is a balance between the bending stiffness and the effective self-affinity in poor solvents. In fact, quite a few single molecule investigations have been conducted on the neutralization mechanism theoretically and experimentally.[31–33] For example, Baumann *et al.*[31] probed the elastic response of single plasmid and lambda phage DNA molecules using optical tweezers at concentrations of trivalent cations. Meanwhile, a reentrant collapsing transition was observed in the elastic response of single DNA molecules at various concentrations of the trivalent cation or spermidine.[32] As for cationic surfactants, the length of their hydrophobic chains plays an important role in their interaction with DNA.[33] On the other hand, fewer investigations have been conducted for the condensing mechanism in poor solvents, of which we know very little. Recently, MacKintosh and coworkers[34,35] predicted that the collapse of semiflexible polymers in poor solvents occurs *via* a series of long-lived, metastable intermediates referred as "tennis racquets". For experimental investigation of the mechanism, ethanol can be a good candidate as it is a poor solvent for DNA and widely used in chemistry, biology and medicine. Ethanol precipitation of DNA is one of the most commonly used procedures in molecular biology.[36–38] Ethanol is a poor solvent for semiflexible DNA, making DNA interactions with its environment less favorable, and DNA tends to be crowded into more compact morphologies. Therefore, the investigation of the interaction between ethanol and DNA may provide insightful information to understand the second condensing mechanism. The morphologies of DNA condensation caused by ethanol have been characterized by a few groups. Fang *et al.*[39] studied the effects of ethanol on the structure of DNA confined to mica in the presence of Mg^{2+} by atomic force microscopy and found a DNA transition from the all-B-form at 0% ethanol to anall-A-form at >25% ethanol. If the specimens are briefly rinsed with anhydrous ethanol, the adsorbed single DNA molecules on mica can subsequently be condensed to toroids and might further collapse into rod-like structures.[40] These observations are supported by the results of dynamic light scattering (DLS) and electronic microscopy.[9] However, few single molecule experimental investigations have focused on this collapse mechanism and dynamics of DNA in poor solvents. The reason might be the much weaker interactions between DNA segments compared with those in multivalent cations and resulting in the difficulty to measure the condensing force. In fact, as a fairly commonly used DNA precipitation agent, the mechanism of DNA condensation induced by ethanol is far from clear. We try to explore this issue in a magnetic tweezers experiment, which is the first single molecule measure for DNA condensation in poor solvents, in order to investigate the exclusion mechanism to the best of our knowledge.

In this paper, single-molecule magnetic tweezer methods and AFM are used to elucidate how ethanol affects DNA condensation. The persistence length of DNA is shown to decrease monotonically with increased ethanol concentration. By exerting a considerably large force, the collapsed DNA can be resolubilized. The decondensation curves show two different elastic behaviors, gradual linear elongation and stepsize jump. This phenomenon can be ascribed as the unzipping of annealed DNA segments and the unlooping of intermediate racquets. AFM imaging revealed many morphologies of DNA, such as flowers, toroids and rods, formed at high concentrations of ethanol. At the vicinity of the critical concentration, the loops by distant crosslinks correspond to the large stepsize jumps in pulling curves, and can be observed in the corresponding AFM images.

2. Experimental details

2.1 Materials

Ethanol was purchased from JingKeHongDa Biotechnology (Shanghai, China). $MgCl_2$ was purchased from Inalco-America Company (Beijing, China). λ phage DNA (48502 bp) for magnetic tweezers experiment and AFM was purchased from New England Biolabs (Ipswich, MA, USA). The stock solution was prepared in 1 × TE buffer (10 mM Tris-HCl (pH = 7.6) and 1 mM EDTA). Solutions were made with 18.2 M Ω deionized water purified through a Milli-Q water purification system (Millipore, Billerica, MA, USA). All agents were used as received and all experiments were repeated at least twice to ensure consistent results.

2.2 DNA construction for single molecule study

For the magnetic tweezers experiments, the λ phage DNA were prepared by covalently attaching 12 bp chemically labeled single-stranded oligonucleotides (3′biotin-cccgccgctgga and 3′digoxygenin (dig) -tccagcggcggg) to their ends as Smith *et al.* did.[41] The DNA molecules were then mixed with 2.8 μm paramagnetic beads coated with strepavidin (M-280, Dynal Biotech) for 15 min to form bead–DNA constructs.[42] DNA molecules carrying a microsphere at one end and dig at the other end were ready for use.

2.3 Magnetic tweezers setup

The measurements were performed using magnetic tweezers, schematically shown in Fig. 1A, similar to the one recently developed by Sun *et al.*[43] A 0.17 mm-thick coverslip with one side polished was sandwiched between two glass slides, which can serve as a flow chamber by sealing the open side of the structure with polydimethylsiloxane. Two 1 mm-diameter holes were made on the top glass slide and linked with a glass capillary to facilitate buffer out or in. The flow chamber was placed on the 40× objective of an inverted microscope. The force exerted on DNA in the focal plane was controlled by a micrometre positioned permanent magnet lateral to the chamber. The polished sidewall was functionalized with anti-dig in order to link with the dig-end of λ-DNA. The DNA–bead construct was then flowed into the cell to form a side wall–DNA–paramagnetic bead structure (Fig. 1B). The distance between the bead and the surface of the sidewall can be deemed as the extension of DNA. The applied force was calculated according to Brownian motions of the microsphere in the direction perpendicular to the DNA extension.[44] Briefly, when the extension is greater than half of DNA contour length, the applied force is determined by $F = k_BT\langle L\rangle/\langle \delta x^2\rangle$, where k_B is Boltzmann's constant, T is temperature, and $\langle L\rangle$ is average extension of single molecules,

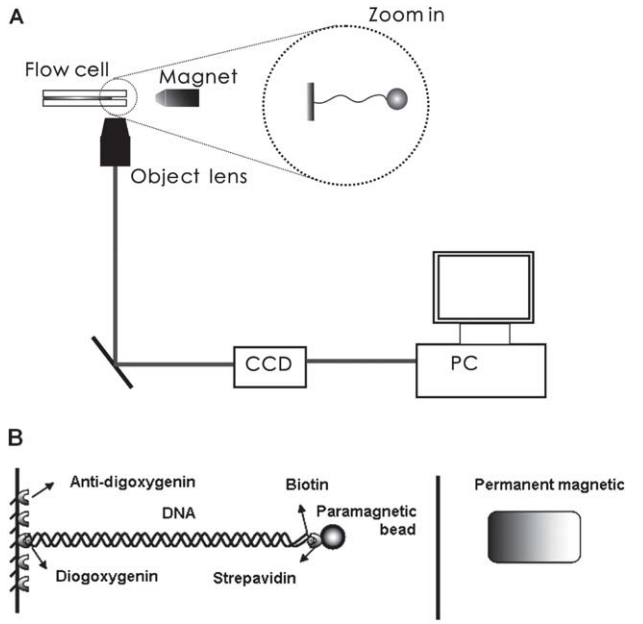

Fig. 1 A. Schematic diagram of magnetic tweezers. B. Bead–DNA–sidewall construct for single molecule experiment.

and $\langle \delta x^2 \rangle$ is the mean square displacement of the bead in the direction perpendicular to the applied force. A video camera was used to monitor the image of the structure in the focal plane and it was used to record the position of the microsphere in real-time. The analysis of the extension was determined by a tracking algorithm by fast Fourier transform-based correlation techniques.[42] After checking a single suspended λ-DNA, diluted ethanol was loaded to the chamber and the elastic response of DNA as a function a time was recorded and analyzed at different forces. The experiments were conducted in phosphate-buffered saline (PBS)(PH = 7.5,140 mM NaCl).

2.4 Single-molecule measurement

The steps of single-molecule experiments are as follows:

(i) Pour the microsphere-bound DNA molecules into the flow cell, then put the cell perpendicularly for 30 min at room temperature, where the polished edge surface of the cover glass is at the bottom of the cell. After the microspheres ligate the polished edge, we rinse the cell with buffer to clean out the free particles.

(ii) Find a ligated particle and confirm that it is connected to the surface through a single DNA molecule.

(iii) Different concentrations of ethanol are injected to the flow cell. Afterwards, remove the magnet so that the DNA molecule can extend with a full flexibility. After incubation for different times, we increase the magnetic force gradually to determine at what force the DNA loop would open. DNA extension was recorded in real-time.

2.5 AFM sample preparation and imaging

Mica pieces (about 1 cm diameter) attached to magnetic steel discs were used as substrates for DNA adsorption. All manipulations were carried out in 1 × TE (10 mM Tris-HCl and 1 mM EDTA pH = 8.0). Actually, PBS and Tris-HCl are two commonly used buffers for DNA storage and dilution. In PBS, DNA has a typical persistence length of ~50 nm similar to the case in physiological condition. However, PBS (PH = 7.5, 140 mM NaCl) contains excess monovalent ions, which may affect the DNA depositing on mica. Thus, TE buffer replaces PBS to be used in AFM sample preparation, as has been used in many AFM studies.[40,45–47]

We studied the change of DNA configuration induced by ethanol through AFM imaging. Experiments were performed in 1 × TE-ethanol solution containing 3.5 mM $MgCl_2$. The concentration of free unmodified DNA was 2.5 ng μl^{-1}. We conducted the experiments at various ethanol concentrations with fixed incubation time and under the fixed concentration condition with different incubation times.

The mixed samples were incubated at room temperature. Then, a drop of 20 μl of the mixture was deposited onto freshly cleaved mica and incubated for 5 min at room temperature. Following the incubation, samples were rinsed with a flow of 20 μl water solution ten times, and then rapidly blown dry using a burst of compressed gas.

The observations were performed with a multi-mode AFM (SPM-9600, Shimadzu, Kyoto, Japan). All AFM imaging was conventional ambient tapping mode AFM, with scan speeds of ~3 Hz and data collection at 512 × 512 pixels. The extension, height, and width of the DNA in AFM imaging were measured manually using off-line analysis software with SPM-9600.

3. Results

3.1 Stretching DNA measurement

A ligated particle was chosen and it was confirmed that it was connected to the surface through a single DNA molecule, where the extension of the λ-DNA should be close to 16 μm under high tension (>10 pN). Then we flew the ethanol–water mixtures at different concentrations to the cell and stretched the DNA by moving the magnet. In contrast with the case of multivalent cations,[20] we cannot observe the compaction of DNA even at very small external force up to 0.2 pN in our experiment when the concentration of ethanol is up to 65%. Thus, the condensation forces are very weak in ethanol. Removing the permanent magnet, we can see that the bead parks near to the sidewall. After incubating the DNA with ethanol for about two hours at room temperature without applied force, we performed constant force unraveling experiments to measure the relation between the extension and pulling time. The results are shown in Fig. 2 and 3. The pulling process was repeatable after removing the permanent magnet and incubating the sample for about two hours again.

Fig. 2 shows the unravelling time course in 30% ethanol but with different applied forces. Such discontinuous jumps were also observed at different forces and concentrations. Fig. 2A, B, C, D show the pulling curves in 30% ethanol, where the corresponding forces are about 0.3 pN, 2.43 pN, 4.3 pN and 6.85 pN respectively. In the single molecule pulling experiment, the displacements of microsphere are in the range of micrometres, corresponding to the change of applied magnetic force less than 0.03 pN. In most cases, errors of the measurement are less than 5%. Therefore, the force can be considered as constant, and needs

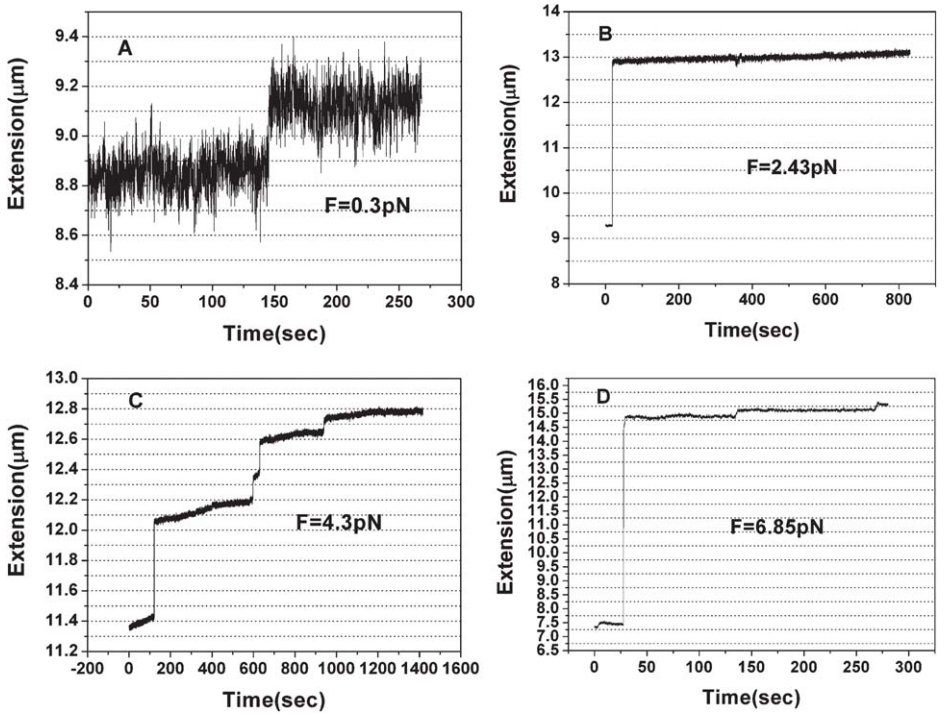

Fig. 2 Unraveling of DNA condensation morphologies at different forces. When the force increased, a series of jumps in DNA extension was observed. The ethanol concentration is 30%.

no further adjustment in the experimental process. The minimal force to induce unravelling steps is quite small. For instance, its value is about 0.3 pN in the case of Fig. 2A. By exerting a considerablly large force, the force–extension curves sometimes show two different elastic behaviors as shown in Fig. 2C, where extension increases with time linearly or jumpily.

Fig. 3 shows the unravelling time course at different concentrations of ethanol at about 1.2 pN force. In Fig. 3A, the ethanol

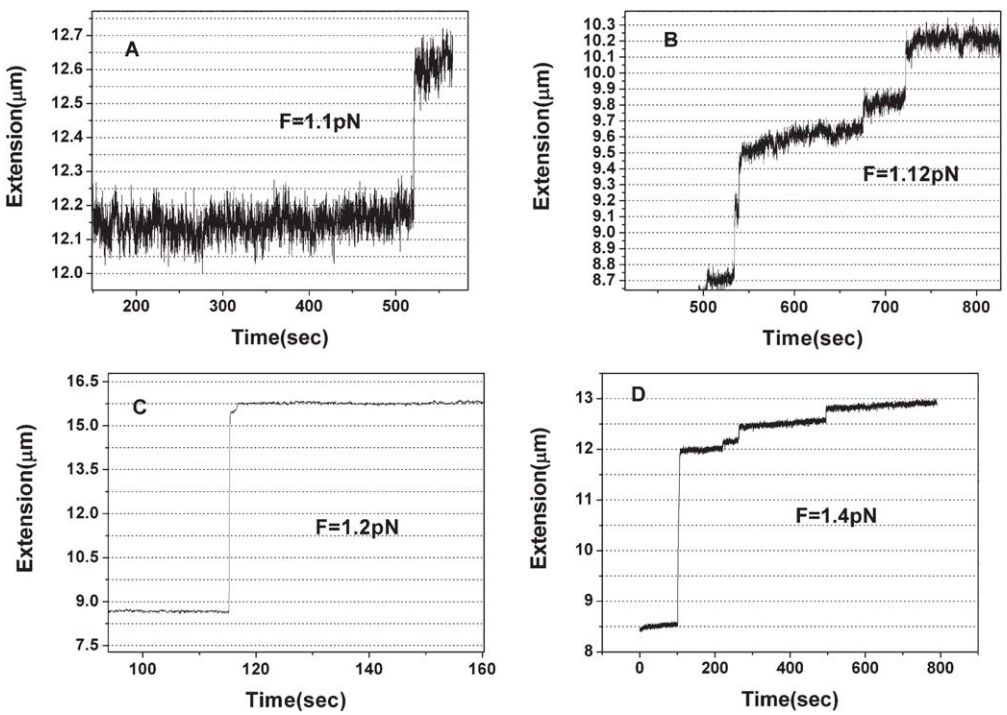

Fig. 3 Unraveling of DNA condensation patterns at different ethanol concentration and the stretching force is near to 1.2 pN. A. The ethanol concentration is 20% at F = 1.1 pN. B. The ethanol concentration is 25% at F = 1.12 pN. C. The ethanol concentration is 30% at F = 1.2 pN. D. The ethanol concentration is 40% at F = 1.4 pN.

concentration is 20% and the pulling force is 1.1 pN. In Fig. 3B, the ethanol concentration is 25% while the force is 1.12 pN. In Fig. 3C, the ethanol concentration is increased to 30% with 1.2 pN external force. When the concentration reaches 40% and the applied force grows a little to 1.4 pN, the pulling curve is shown in Fig. 3D.

The condensation forces are very weak in ethanol. We cannot observe the compaction of DNA at very small applied force in our experiment when the concentration of ethanol is up to 50% as shown in Fig. 4. In Fig. 4A, the applied force is about 0.52 pN and the ethanol concentration is 50% and the extension of the DNA is kept at 10.12 μm in the observation duration or longer. Actually, the incubation time in Fig. 4 is nearly the same as that in Fig. 2A. No compaction occurs throughout the incubation time for up to 2 h with a small load force. When we lowered the force to as low as 0.2 pN, there was still no shrinking compared with the case in multivalent cations although the fluctuation increased significantly. In other words, DNA can only condense in ethanol in the absence of a pulling force. When a small pulling force (even less than that in the unravelling process) is applied, which is case of Fig. 4, DNA in ethanol could not condense or compact even when it is incubated for a long time (more than 2 h). Therefore, for DNA in ethanol, the unravelling is not a reversible process of the condensing.

Fig. 5A shows the distribution of unravelling step sizes. The peak of the distribution of step sizes induced by ethanol is centered 70 ± 10 nm (average of 100 step sizes), which is much smaller than that induced by multivalent cations.[20] This observation suggests more subtle structures or intermediate states existing in the system rather than the typical toroids. We ascribe the peak of 70–80 nm to the irregular racquets in theoretical simulations.[34,48] However, we could still see distinct jumps; besides the 70 nm jumps, many jump sizes are less than 70 nm. At the same time, >400 nm jumps could be seen. In our experiments, we also found very large jumps at different concentrations. Their step sizes are about a few microns. Fig. 3C shows a big jump in 30% ethanol. The extension of step size is around 7 μmat F = 1.2 pN. To observe more directly large jumps on DNA structures, we then used AFM scanning to image DNA in the presence of 30% ethanol in Fig. 5B. We can see that the DNA can form many loops on a mica surface. This observation provides some evidence for single molecule pulling.

3.2 AFM images of DNA condensation

To observe more directly the effect of ethanol on DNA morphologies, we used AFM scanning to image DNA in the presence of different concentrations of ethanol and also observed the change of DNA morphologies at different moments. AFM may modify the actual morphology of DNA in ethanol solution. However, the condensed DNA is adsorbed on a mica surface and only binds to the surface loosely. Balhorn *et al.*[49] showed that treatment of DNA adsorbed to a surface with a solution of multivalent cations produced toroids with lateral dimensions

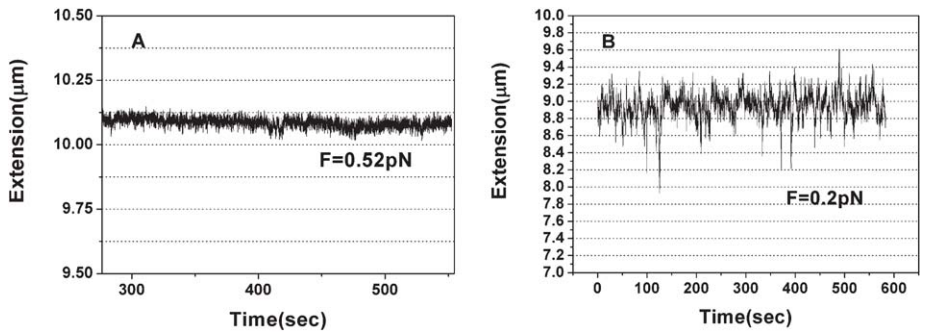

Fig. 4 The extension–time curves of stretching DNA in 50% ethanol. A. When the force decreased at 0.52 pN, the extension is about 10.12 μm after 6 min. B. When the force is 0.2 pN, the extension is about 8.94 μm after 10 min.

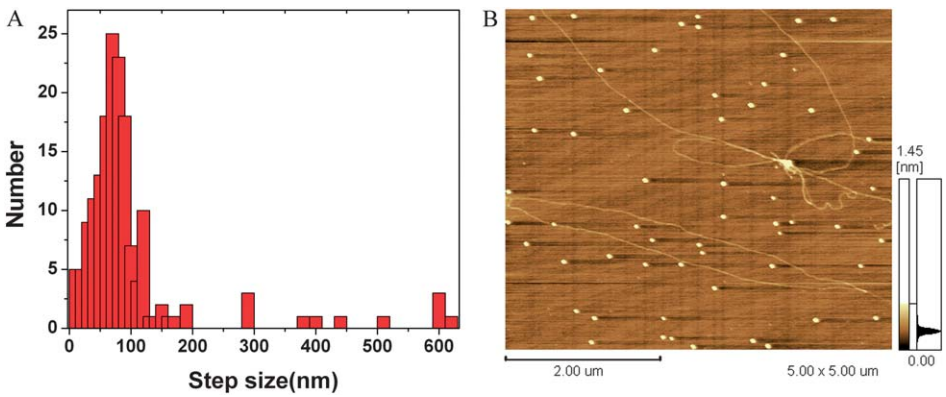

Fig. 5 A. Corresponding histograms of the step size in all of the ethanol concentrations. B. AFM image of big DNA loops of condensation morphologies by 30% ethanol.

(*i.e.* diameters) similar to those in solution but with smaller heights (the axial direction). Thus, AFM images are flattening morphology of DNA condensates with their original compacting structure.

Using the method described in the materials and methods section, the mixed liquor of samples was incubated at room temperature for 1 h. λ-DNA molecules were fully extended and had few loops by bending. We do not see the condensation kinks (Fig. 6A).

In the presence of 15% ethanol, some local kinks appeared. We may see many loops by DNA kinking (Fig. 6B). When the concentration of ethanol is about 30%, the morphologies of flowers were observed by AFM (Fig. 6C). The flower patterns have cores in the middle which are formed by the crossovers of many DNA molecules; the remaining DNA segments wrap the core loosely. When the concentration of ethanol is increased to 60%, we can see the toroid morphologies on the mica surface in Fig. 6E. Besides toroids, we also have observed rod-like condensed structures in Fig. 6*E*-1 (inset of Fig. 6E). More compact globular structures appeared in high concentration of ethanol (Fig. 6F). However, the typical toroidal morphology is difficult to see on mica surface in our experiment. Many of the morphologies were flowers as shown in Fig. 6D.

We incubated λ-DNA with 50% ethanol for different times in advance, then used it for AFM sample operation. The morphologies of DNA on mica surface would change with time in Fig. 7. The incubation time is 10 min, 30 min, 1 h, 2 h, 3 h, 5 h respectively.

In the presence of 50% ethanol, after incubation of 10 min, some small loops appeared in Fig. 7A. When incubation time increased, these loops developed further as shown in Fig. 7B, 7C, 7D (30 min, 1 h, 2 h). When incubation time reached 3 h we can observe the flowers' morphologies as shown in Fig. 7E. If the incubation time is 5 h, a more compact pattern formed on the mica surface as shown in Fig. 7F. However, as the ethanol concentration is increased to 80% and the time of incubation is about 10 h, a range of more complex pancake and snowflake structures appeared as shown in Fig. 8.

4. Discussion

4.1 Persistence length as a function of ethanol concentration

The persistence length and contour length of DNA can be obtained by fitting the force *versus* DNA extension curves with the worm-like chain (WLC) model,[50]

$$F = \frac{K_B T}{A}\left[\frac{1}{4\left(1-\langle L\rangle/L_0\right)^2} - \frac{1}{4} + \frac{\langle L\rangle}{L_0} + \sum_{i=2}^{i\leq 7}\alpha_i\left(\frac{\langle L\rangle}{L_0}\right)^i\right] \quad (1)$$

where F is the stretching force, L is the DNA extension, A and L_0 are the persistence length and the contour length of the DNA molecule.

In PBS buffer, by fitting the data of force *versus* extension measurement with the WLC model, a persistence length of λ-DNA should be 52 ± 2 nm and a contour length should be at 16.5 ± 0.5 μm. We carried out the WLC behavior measurement of DNA condensed by ethanol at different concentrations. First, we flew ethanol at a given concentration to the flow cell. Next, we adjusted the applied force and recorded the position of the microsphere in real-time. The DNA persistence length in the presence of different concentrations of ethanol was extracted by fitting the stretching data with the appropriate WLC models.

Fig. 9A shows typical force–extension curves for DNA interacting with 30% and 50% ethanol for two hours. The corresponding WLC model fitted persistence lengths are shown in Fig. 9B. We can see that the persistence lengths decrease

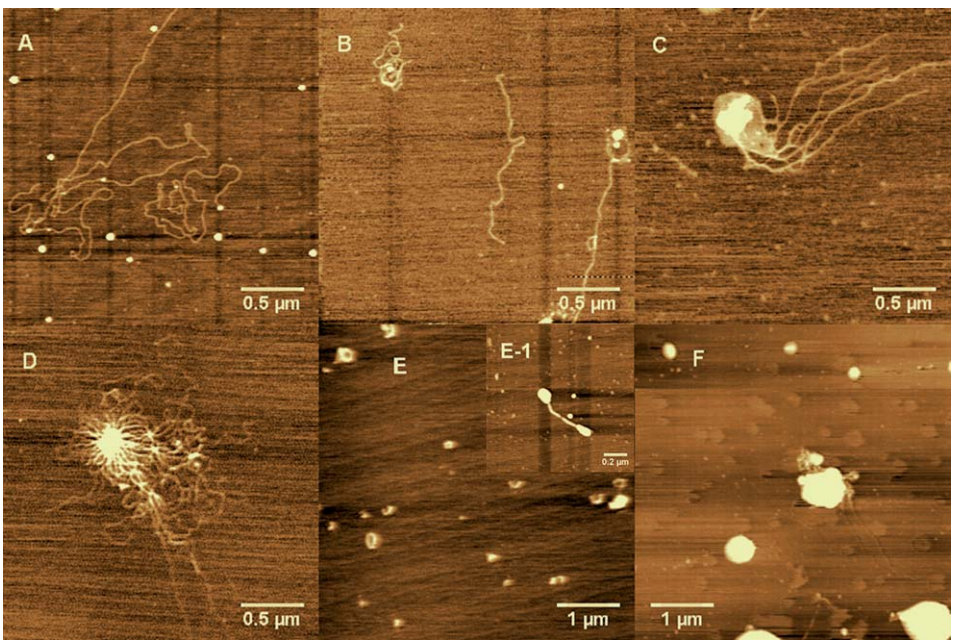

Fig. 6 AFM images of λ-DNA alone or incubated with ethanol at different concentrations. (A) Unmodified DNA in the absence of ethanol. The DNA was freely extended. (B–F) In the presence of 15% ethanol, 30% ethanol, 50% ethanol, 60% ethanol and 80% ethanol. DNA was condensed by ethanol to more racquets, flowers, toroids, rods and compacted globules.

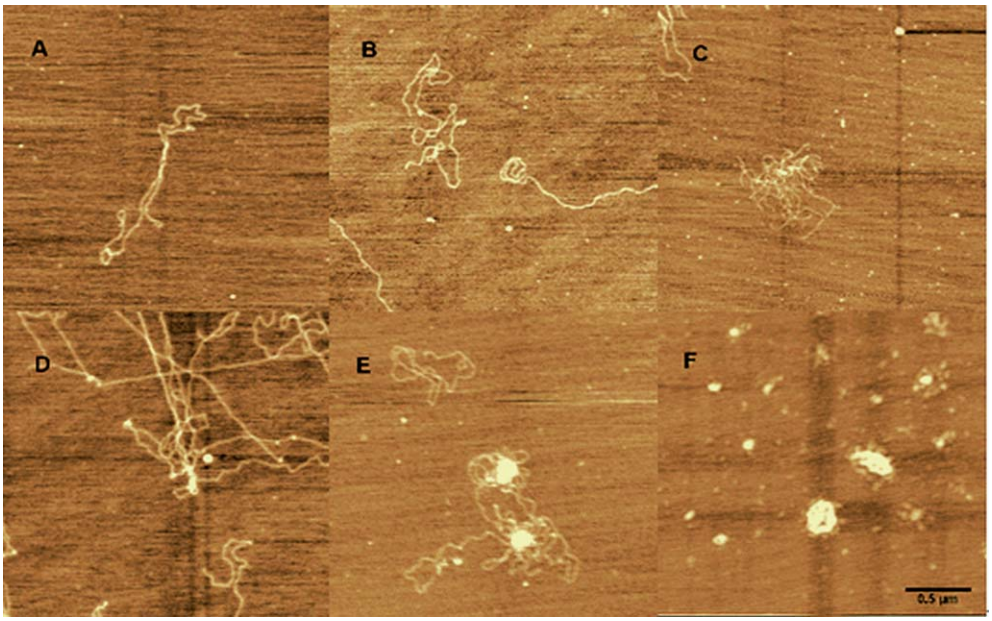

Fig. 7 A–F images represent a range of intermediates of condensed λ-DNA in 50% ethanol at different times. A very wide range of structures is seen at any given ethanol concentration, particularly at higher concentrations. The scale bar is 0.5 μm.

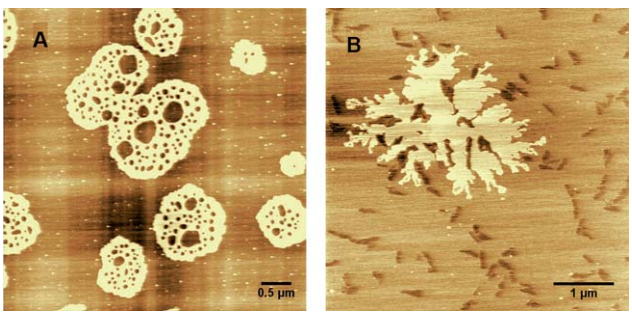

Fig. 8 Condensed lambda-DNA in 80% ethanol and with a time of incubation of about 10 h. A range of more complex pancake and snowflake structures appear.

monotonically with increasing ethanol concentration. When the concentration of ethanol is 30%, the persistence length is about 25 nm. When the concentration exceeds 50%, the persistence length is below 15 nm. However, when the concentration of ethanol is higher than around 70%, the single DNA tends to precipitate and the measurement can not be achieved.

The persistence length is an important parameter, which characterizes the flexibility of linear macromolecules. DNA can be treated as a semi-flexible chain, and its flexibility is reflected by the persistence length. The persistence length of high-molecule-weight DNA has been measured in the presence of low concentration of multivalent cations by methods as diverse as linear dichroism and intrinsic viscosity,[51] electrooptical techniques,[52] and stretching of single DNA molecules by laser tweezers.[4] The persistence length of DNA on the mica can be determined from AFM images of individual DNA molecules,[39] where the

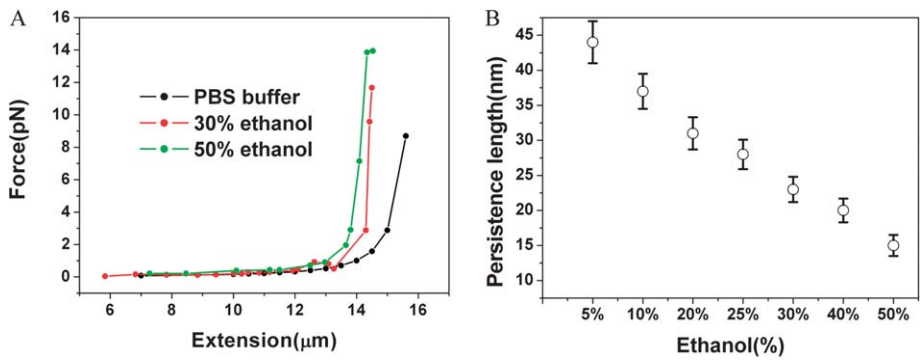

Fig. 9 A. Response of single λ-DNA molecules to applied forces with condensing concentrations of the ethanol. The molecule in a monovalent salt background buffer displayed a WLC model with P = 52 nm and L = 16.5 μm. Upon addition of either 30% or 50% ethanol to this solution, the λ-DNA molecule displayed high force entropic elasticity indicative of a WLC with increased chain flexibility (p < 50 nm). B. Persistence length of DNA as a function of ethanol concentration.

persistence length was determined by measuring the dependence of the angle between two segments (at an arbitrary position on the molecule) on the extension of the segment. For a single λ-DNA molecule, previous experiments revealed a persistence length of 45–50 nm and a contour length of about 16.5 μm. In our experiment, we found that its contour length decreases gradually from its value in buffer with the ethanol concentration.

We performed the force *versus* extension measurements as shown in Fig. 9A. When a force larger than 5 pN is applied, all the compacted structures are unwound and the chain approaches its contour length. We can see that its contour length in ethanol solution is less than the value in the PBS buffer. We can ascribe this feature to the B–A transition as observed by Hoh's group,[39] in which the rise per base pair decreases from 3.4 angstroms for B-form to 2.6 angstroms for A-form. In the B-form, the contour length increases slowly with the applied force. However, in the A-form, it keeps almost constant with increasing pulling force. We can conclude that tensile modulus of A-form DNA is larger than the value of B-form.

By introducing ethanol at different concentration to DNA solution, we studied the concentration dependence of DNA persistence length. From fitting of the curves with eqn (1), we found that persistence lengths decrease monotonically as the concentration of ethanol increase as shown in Fig. 9B. Because of the very week attractive interactions between DNA segments in ethanol solution, indeed, we can not see the differences in the initial linear regime among these three conditions. However, when their extensions reach about 2/3 (12 μm) of the corresponding contour lengths, we can see in Fig. 9A the different slopes in the force–extension curves due to the changing persistence length of DNA in ethanol solution. As for the last regime, the much sharper slopes correspond to the DNA elastic response to applied force near reaching their contour lengths.

4.2 Stretching DNA

In a poor solvent, semiflexible biopolymers such as DNA and F-actin attempt to avoid contact with the solvent and hence collapse into compact structures to minimize their surface areas. They are usually characterized by large cross-sectional areas or complex multi-backbone internal structure, which in turn implies a strong resistance to bending and causes spherical globules to be energetically disfavored. The apparent equilibrium states for these polymers have been shown to be rings and toroids when such chains immersed in a poor solvent, or in the presence of a compensating agent.[9,16,53] However, the process of collapse to the final energy minimum state may undergo a series of intermediate states, which is the main concern of the present investigation.

In order to measure the nucleation of intramolecular collapse in a stretched DNA chain, we pulled the DNA at very low force to observe its collapse, as shown in Fig. 4A (at 50% ethanol concentration and 0.52 pN pulling force) and Fig. 4B (at 50% ethanol concentration and 0.2 pN pulling force). In two hours, we didn't observe the compaction of DNA with the small load force. These results are different from cases of multivalent cations and surfactants,[20,31,33] where such compaction can be easily observed due to the first-order transition of unfolding to folding.[20] We can infer there is no such first-order transition occurring the when DNA is in an ethanol solution, which suggests that DNA condensing in ethanol is *via* an annealing mechanism between segments rather than charge neutralization correlation effect. When the small force is removed and the DNA is incubated with the ethanol solution for a long time of about two hours, the unravelling experiments can proceed again with typical pulling curves.

In our unravelling experiments, the minimal pulling force to unwind the collapsed single DNA molecule is less than 1 pN. In contrast with the almost uniform pulling steps in the case of multivalent cations, the current staircase pulling curves are irregular and hysteretic. It was observed that almost all DNA molecules exhibited shorter extension than their values in PBS buffer at the same force. It might be ascribed to the A–B transition of DNA structure as described in ref. 39. Several elements of DNA's structure are important to racquets or toroid formation: its charge density, its stiffness, and its large extension-to-width ratio. To study the mechanical properties of the condensed DNA, we performed constant force unravelling experiments. Many jumps occur at the corresponding forces and most of the jump sizes are less than 80 nm. Sometimes, we found big steps in different concentrations of ethanol. Their step sizes can reach a few microns as shown in Fig. 3C, where the size of a step is around 7 μm at $F = 1.2$ pN at 30% ethanol concentration. As we mentioned, the condensing force induced by ethanol is very weak. Therefore, we have to incubate the DNA sample with ethanol for quite long time to form condensed structures. In the process, distant contacts and crosslinks can be formed because of solvent exclusion. The step jumps spanning a larger range correspond to the unfolding of these kinds of loops or loose racquet heads. In the AFM image shown in Fig. 5B, we observe large DNA loops. This means that the large jumps in the pulling experiments correspond to the unfolding of a big loop or loose racquet head of DNA induced by ethanol. We think that our observation corresponds to the combination of the toroid patterns as shown in Fig. 10C and the racquet heads as shown in Fig. 10B. In contrast with the case of multivalent cations, it seems that there is no correlation between the force and jump steps. In a multivalent cationic solution, large staircases in pulling curve may represent two or more turns of DNA unwrapped from the

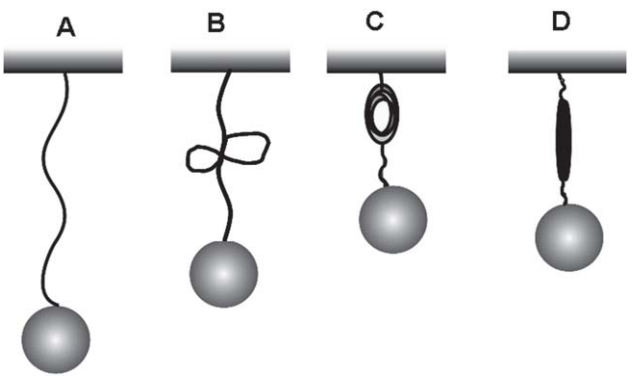

Fig. 10 A. The distance between the bead and the surface of the sidewall can be deemed as the extension of DNA. B. When the ethanol was added to the DNA solution, the structures of racquets occurred. C. Some other toroid morphologies were formed by DNA condensation. D. The morphologies of rods were formed in DNA condensation too.

same toroid at the same time. But the micron-jumps induced by ethanol may represent the racquet patterns unwrapped from the crossover points. Since there are so many condensed morphologies and intermediate states, we modeled these features as shown in Fig. 10.

We can understand some of the features observed in our experiments in terms of a simple model for dynamical intermediates developed by MacKintosh *et al.*[7,35,48] In contrast to the mechanism for flexible chains, they suggest that the collapse occurs *via* a series of long-lived, metastable intermediates referred as "tennis racquets". These intermediates form a well-defined, hierarchical family of conformations. The collapsed state configuration and pathways to their formation are the result of the interplay between two opposing forces: the bending force related to the chain stiffness and the attractive force due to the poor solvency of the environment. Ishimoto *et al.*[54] have similar results and have shown that the *meta*-state racquet states appear as the classical solutions of the low-energy effective theory of a semiflexible homopolymer chain. From the extension–time curves we can see that the step sizes are from tens of nanometres to a few micrometres. In Fig. 5A, we can see that the peak of the distribution of step sizes is centered about 70–80 nm, and a long tail exists up to 600 nm. We ascribe the peak of 70–80 nm to the unwrapping of minimal DNA racquet heads while the long tail to the loose DNA loops or irregular racquet structures.

Brownian Dynamics (BD) simulations have found a seemingly generic pathway of collapse for semiflexible polymers, *via* long-lived metastable "racquet" states, so named for their resemblance to tennis racquets (see Fig. 10B). These simulation results motivated a theoretical study of toroid and racquet conformations, which found toroids to be the ground state of the system (as well as the rod at short enough contour lengths) with a series of metastable racquet solutions at higher energies, in agreement with the simulation results.[34] As we can see from Fig. 2 and 3, a jump in pulling curve correspond to an unfolding of the racquet head or the loop of the toroid. In addition, there are a lot of linear elongations of the collapsed DNA between two step-like jumps in the curves. We ascribe the linear elongations to the unzipping of the annealed racquet handles. Because of the existence of ethanol, the attractive potential between DNA segments leads them to bind together. When the external load force F is larger than a critical value, the annealed DNA segments are separated again. We calculated 25 linear extension parts in pulling curves to estimate the attractive energy per monomer at different ethanol concentrations. The attractive energies at 30% and 50% ethanol concentration are about $0.2k_BT$ and $0.26k_BT$ per persistence length, which yield unbinding forces of about 0.3 pN and 0.4 pN, respectively.

4.3 Analysis of morphologies of ethanol-induced DNA condensates

As we have seen in the single molecule pulling experiments, the attraction between DNA segments due to exclusion are very weak. Therefore, we have to incubate the DNA and ethanol for a quite long time to anneal them. In our experiments, we can see the condensation morphologies of the DNA with a general tendency for increasing looped and complex structures with increasing ethanol concentration, which is consistent with the results of previous AFM experiments.[39,40] As in ref. 39, we incubated lambda DNA in ethanol solution rather than rinsing the specimen with anhydrous ethanol as in ref. 40. In the absence of ethanol, the DNA molecules are well separated on the surface, and have relaxed morphologies with no condensation loops, as shown in Fig. 6A. At lower ethanol concentrations, there are few intermolecular contacts, but individual molecules have an increased number of intramolecular loops with increasing ethanol concentration. At ethanol >15%, multi-molecular complexes appear, including ones with the flower patters composed of many racquets. These flowers are highly looped with one or more crossover points. There is a general tendency for the structures to become more complex and compact with increasing ethanol concentrations. Similar to the results obtained when the specimen was rinsed by anhydrous ethanol, sometimes the condensation morphology is a toroid as shown in Fig. 7E. Since DNA is a semiflexible polymer molecule and the attractive forces between DNA segments are rather weak, the DNA molecules in poor solvent tend to form compact toroidal structures in solution due to the equilibrium between the exclusion and bending energy. Besides toroids, a small fraction of rod-like structures can be also observed. The rod-like structures might be formed by a side-by-side collapse of the inner (nucleation) loop of the larger toroidal structures. At the highest concentrations of ethanol ($\sim$70%), we can see some even more compacting patters such as globules on a mica surface. At a high concentration of ethanol and under carefully controlled conditions it can produce particles of a well defined morphology, and can be used to precipitate DNA.[36,37] Many other structures appear on the surface of mica if the incubation time is long enough, for example, flat pancakes and snow flakes as shown in Fig. 8. There is a strong variation in shape, height, and spread of the absorbed DNA molecules, which can be attributed to the competing DNA-surface and solvent interaction in the pathway controlled condensation process. These kinds of DNA morphologies are consistent with our single molecular pulling experiments where the racquet structures are unravelled one by one.

5. Conclusions

We have used magnetic tweezers and AFM to investigate the single DNA molecule condensation induced by ethanol. With the increasing concentration of ethanol, the persistence length of DNA decreased monotonically. We have observed more extensive condensation structures compared with previous studies.[39] Most of them are irregular racquets, which are much looser than those induced by multivalent cations. Single molecule pulling experiments have shown that the condensation forces between DNA segments in ethanol solution are much weaker than those in a solution of multivalent cations. The tensile modulus of DNA is also increased with the transition from B-form to A-form. These observations suggest that the condensation of DNA in ethanol is *via* a series of metastable racquet intermediates to final toroids described by the collapse model of semiflexible polymers in poor solvents while the condensation by multivalent cations is based on much stronger charge neutralization mechanism of backbones.

Acknowledgements

This work is partially supported by the National Natural Science Foundation of China (Grant No. 10974146 and 20934004) and Zhejiang Provincial Natural Science Foundation (Grant No. Y6090222).

References

1 R. Balhorn, M. Cosman, K. Thornton, V. V. Krishnan, M. Corzett, G. Bench, C. Kramer, N. V. Hud, M. Allen and M. Prieto, in *The Male Gamete: From Basic Science to Clinical Applications*, Cache River Press, Clearwater, Florida, 1999, 55–70.
2 M. E. Cerritelli, N. Cheng, A. H. Rosenberg, C. E. McPherson, F. P. Booy and A. C. Steven, *Cell*, 1997, **91**, 271–280.
3 R. I. Mahato, Y. Takakura and M. Hashida, *Critical reviews in therapeutic drug carrier systems*, 1997, **14**, 133.
4 C. Baumann, S. Smith, V. Bloomfield and C. Bustamante, *Proc. Natl. Acad. Sci. U. S. A.*, 1997, **94**, 6185.
5 V. Bloomfield, *Curr. Opin. Struct. Biol.*, 1996, **6**, 334–341.
6 N. V. Hud and I. D. Vilfan, *Annu. Rev. Biophys. Biomol. Struct.*, 2005, **34**, 295–318.
7 B. Schnurr, F. MacKintosh and D. Williams, *Europhys. Lett.*, 2000, **51**, 279–285.
8 Z. Ou and M. Muthukumar, *J. Chem. Phys.*, 2005, **123**, 074905.
9 P. G. Arscott, C. Ma, J. R. Wenner and V. A. Bloomfield, *Biopolymers*, 1995, **36**, 345–364.
10 T. Kundu and M. Rao, *Biochemistry*, 1995, **34**, 5143–5150.
11 L. Lerman, *Proc. Natl. Acad. Sci. U. S. A.*, 1971, **68**, 1886–1890.
12 L. Murphy and S. Zimmerman, *Biochim. Biophys. Acta, Gene Struct. Expression*, 1994, **1219**, 277–284.
13 L. Murphy and S. Zimmerman, *Biophys. Chem.*, 1995, **57**, 71–92.
14 D. Louie and P. Serwer, *J. Mol. Biol.*, 1994, **242**, 547.
15 S. Zimmerman and A. Minton, *Annu. Rev. Biophys. Biomol. Struct.*, 1993, **22**, 27–65.
16 V. Vasilevskaya, A. Khokhlov, Y. Matsuzawa and K. Yoshikawa, *J. Chem. Phys.*, 1995, **102**, 6595.
17 H. Farhood, X. Gao, K. Son, Y. Yang, J. Lazo, L. Huang, J. Barsoum, R. Bottega and R. Epand, *Ann. N. Y. Acad. Sci.*, 1994, **716**, 23.
18 P. Felgner, T. Gadek, M. Holm, R. Roman, H. Chan, M. Wenz, J. Northrop, G. Ringold and M. Danielsen, *Proc. Natl. Acad. Sci. U. S. A.*, 1987, **84**, 7413.
19 X. Hou, X. Zhang, K. Wei, C. Ji, S. Dou, W. Wang, M. Li and P. Wang, *Nucleic Acids Res.*, 2009, **37**, 1400.
20 W. Fu, X. Wang, X. Zhang, S. Ran, J. Yan and M. Li, *J. Am. Chem. Soc.*, 2006, **128**, 15040–15041.
21 K. Besteman, S. Hage, N. Dekker and S. Lemay, *Phys. Rev. Lett.*, 2007, **98**, 58103.
22 B. Ali, R. Amit, I. Braslavsky, A. Oppenheim, O. Gileadi and J. Stavans, *Proc. Natl. Acad. Sci. U. S. A.*, 2001, **98**, 10658.
23 R. Amit, A. Oppenheim and J. Stavans, *Biophys. J.*, 2003, **84**, 2467–2473.
24 J. van Noort, S. Verbrugge, N. Goosen, C. Dekker and R. Dame, *Proc. Natl. Acad. Sci. U. S. A.*, 2004, **101**, 6969.
25 M. Shen, K. Downing, R. Balhorn and N. Hud, *J. Am. Chem. Soc.*, 2000, **122**, 4833–4834.
26 C. Conwell, I. Vilfan and N. Hud, *Proc. Natl. Acad. Sci. U. S. A.*, 2003, **100**, 9296.
27 A. Zinchenko, V. Sergeyev, S. Murata and K. Yoshikawas, *J. Am. Chem. Soc.*, 2003, **125**, 4414–4415.
28 N. Chen, A. Zinchenko, S. Murata and K. Yoshikawa, *J. Am. Chem. Soc.*, 2005, **127**, 10910–10916.
29 C. Baumann, V. Bloomfield, S. Smith, C. Bustamante, M. Wang and S. Block, *Biophys. J.*, 2000, **78**, 1965–1978.
30 V. A. Bloomfield, *Biopolymers/Nucleic Acid Sci.*, 1998, **44**, 269–282.
31 C. G. Baumann, V. A. Bloomfield, S. B. Smith, C. Bustamante, M. D. Wang and S. M. Block, *Biophys. J.*, 2000, **78**, 1965–1978.
32 Y. Murayama, Y. Sakamaki and M. Sano, *Phys. Rev. Lett.*, 2003, **90**, 18102.
33 S. Husale, W. Grange, M. Karle, S. Burgi and M. Hegner, *Nucleic Acids Res.*, 2008, **36**, 1443.
34 B. Schnurr, F. Gittes and F. C. MacKintosh, *Phys. Rev. E: Stat. Phys., Plasmas, Fluids, Relat. Interdiscip. Top.*, 2002, **65**, 61904.
35 A. Montesi, M. Pasquali and F. C. MacKintosh, *Phys. Rev. E: Stat., Nonlinear, Soft Matter Phys.*, 2004, **69**, 21916.
36 C. Gaillard and F. Strauss, *Nucleic Acids Res.*, 1990, **18**, 378.
37 K. R. Paithankar and K. S. Prasad, *Nucleic Acids Res.*, 1991, **19**, 1346.
38 M. Tom, in *DNA–protein interactions: principles and protocols,* Humta Press, Totowa, New Jersey, 2004, vol. 148, p. 4.
39 Y. Fang, T. Spisz and J. Hoh, *Nucleic Acids Res.*, 1999, **27**, 1943.
40 C. Zhang and J. van der Maarel, *Journal of Physical Chemistry B-Condensed Phase*, 2008, **112**, 3552–3557.
41 S. Smith, L. Finzi and C. Bustamante, *Science*, 1992, **258**, 1122.
42 T. Strick, J. Allemand, D. Bensimon and V. Croquette, *Biophys. J.*, 1998, **74**, 2016–2028.
43 B. Sun, K. J. Wei, B. Zhang, X. H. Zhang, S. X. Dou, M. Li and X. G. Xi, *Nature*, 2008, **27**, 3279–3287.
44 J. Yan, D. Skoko and J. Marko, *Phys. Rev. E: Stat., Nonlinear, Soft Matter Phys.*, 2004, **70**, 11905.
45 V. Andrushchenko, Z. Leonenko, D. Cramb, H. van de Sande and H. Wieser, *Biopolymers*, 2002, **61**, 243–260.
46 C. C. Conwell and N. V. Hud, *Biochemistry*, 2004, **43**, 5380–5387.
47 M. J. Allen, E. M. Bradbury and R. Balhorn, *Nucleic Acids Res.*, 1997, **25**, 2221.
48 B. Schnurr, F. C. MacKintosh and D. R. M. Williams, *Europhys. Lett.*, 2000, **51**, 279.
49 M. Allen, E. Bradbury and R. Balhorn, *Nucleic Acids Res.*, 1997, **25**, 2221.
50 C. Bouchiat, M. Wang, J. Allemand, T. Strick, S. Block and V. Croquette, *Biophys. J.*, 1999, **76**, 409–413.
51 W. A. Baase, P. W. Staskus and S. A. Allison, *Biopolymers*, 1984, **23**, 2835–2851.
52 R. Marquet and C. Houssier, *Journal of biomolecular structure & dynamics*, 1988, **6**, 235.
53 W. M. Gelbart, R. F. Bruinsma, P. A. Pincus and V. A. Parsegian, *Phys. Today*, 2000, **53**, 38.
54 Y. Ishimoto and N. Kikuchi, *J. Chem. Phys.*, 2006, **125**, 074905.

